A Novel and Facile Method for the Synthesis of Octa(aminophenyl)silsesquioxane and Its Nanocomposites with Bismaleimide-Diamine Resin

Jun Zhang, Ri-Wei Xu, Ding-Sheng Yu

College of Materials Science and Engineering, Beijing University of Chemical Technology, Beijing 100029, China

Received 3 March 2006; accepted 9 July 2006
DOI 10.1002/app.25290
Published online in Wiley InterScience (www.interscience.wiley.com).

ABSTRACT: Octa(aminophenyl)silsesquioxane (OAPS) was prepared from octa(nitrophenyl)silsesquioxane (ONPS) by using the stable, inexpensive, and readily available hydrazine hydrate as the reducing agent with a yield of around 86%. The product was characterized by FTIR, GPC, ^{1}H NMR, ^{29}Si NMR, and XRD. It was found that the time period for preparation of ONPS from octaphenylsilsesquioxane could be considerably shortened, reaching the complete nitration and avoiding double nitration of the aromatic rings. The polyimides were prepared by the reaction of *N*,*N*′-bismaleimido-4,4′-diphenylmethane with OAPS and 4,4′-diamino-diphenyl ether. The structure of resulting organic–inorganic hybrid nanocomposites was characterized by XRD and FTIR. The decomposition temperature and char yield of resulting materials increased with increasing OAPS loading. The DSC data showed that the glass transition temperature of nanocomposite was enhanced by 36°C with the content of OAPS around 15 wt %. As the feed amount of OAPS increased further, the decrease in T_g's could be observed. © 2006 Wiley Periodicals, Inc. J Appl Polym Sci 103: 1004–1010, 2007

Key words: hydrazine; nanocomposite; octa(aminophenyl)silsesquioxane; polyimide; octa(nitrophenyl)silsesquioxane

INTRODUCTION

Polyhedral oligomeric silsesquioxanes (POSS) have emerged as a new class of chemical feedstock for developing nanoreinforced organic–inorganic hybrid materials with excellent properties.[1–8] POSS macromonomers are relatively large molecules containing inorganic cores surrounded by organic groups. These macromonomers have been used to prepare many thermoset organic–inorganic hybrid nanocomposites with attractive properties, such as excellent mechanical properties, thermal stability, and flame retardation.[3,5–7,9–13] In these composites, the cubic silica cores are defined as ''hard particles'' with a 0.53 nm diameter and a spherical radius of 1–3 nm including the functionalized organic arms and can be monodispersed.[14]

Among various POSS macromonomers, the octa-(aminophenyl)silsesquioxane (OAPS), which possesses the structure of cube-octameric framework with eight corner amine groups, is the most interesting one. It is not only because of high temperature stability of inorganic cube, but also due to the various functional groups that can be derived from the amine groups of OAPS. Thus, OAPS provides limitless opportunities for manipulating/tailoring nanocomposite properties.[9,14–17] However, OAPS is expensive, which limited its application. So far, OAPS have been prepared by nitration of octaphenylsilsesquioxane (OPS) to form octa(nitrophenyl)silsesquioxane (ONPS), followed by hydrogen-transfer reduction using Pd/C as the catalyst giving a yield of around 82%.[9,10] The use of OAPS in modification of polymers has been increasing recently. Laine and coworkers[14,18,19] has studied some thermoset organic–inorganic hybrid composites based on OAPS. Their results showed that cubic silsesquioxane-modified polymers possess high compressive strength and thermal stability.

Bismaleimide resins have been widely used as matrices in the aerospace and aeronautic industries because of their good performances such as temperature stability, hot–wet strength, low cost, and maintain the epoxy-like processing ability. The unsaturated end groups of bismaleimide can be polymerized thermally without the formation of volatile by-products, offering considerable advantages in processing over the conventional condensation type polyimides. However, the major drawback of bisamleimide resins is the brittleness. One of the most important methods for modifying bismaleimide resins is the use of a coreactant, such as diamine. The introduction of longer segments of diamine between the crosslinking points could reduce the brittleness of the polyimides, but might reduce the glass transition temperature of polyimides.[20–22]

Correspondence to: D.-S. Yu (yuds@mail.buct.edu.cn).
Contract grant sponsor: National Nature Science Foundation of China; contract grant number: 50473041.

Considering the importance of OAPS in developing high-performance nanocomposites, we report here a novel and facile way for the preparation of OAPS by using the stable, inexpensive, and readily available hydrazine hydrate as the reducing agent, offering a low cost alternative to the Pd/C catalyst. In addition, polyimide nanocomposites by Michael addition reaction of OAPS and diamine with bismaleimide were prepared. The thermal properties and flame retardence of resulting nanocomposites were investigated.

EXPERIMENTAL

Materials

OPS was obtained from Aldrich and *N*,*N*′-bismaleimido-4,4′-diphenylmethane (BMI) was provided by Honghu Bismaleimide Resin Factory, China. Hydrazine hydrate (80%) was purchased from the Tianjin Kermel Chemical Reagents Development Centre, Tianjin. 4,4′-Diaminodiphenylether (DDE) was provided by Shanghai 3S Reagent THF, ethyl acetate, fuming nitric acid, acetone, $FeCl_3$, and active charcoal powder were of analytical reagent grade and purchased from Beijing Chemical Reagent Company. THF was dried over molecular sieves and distilled over CaH_2. Acetone was purified by distillation and dried over molecular sieves. Other chemicals mentioned earlier were used without further purification.

Synthesis of ONPS

ONPS was synthesized by following Laine and coworkers' method[10] with the modification of shortened nitrifying time from 20 to 6 h. The yield of the yellow ONPS was 92%.

FTIR (KBr): 1350 (s; N═O), 1529 (s; N═O), 1100 (s; Si—O—Si); ^{29}Si solid NMR (δ, ppm): −79.5, −82.8; ^{1}H NMR (acetone-d_6) (δ, ppm): 8.7 (t, 1.0H), 8.5–8.0 (m, 4.2H), 7.8 (m, 2.7H); GPC: M_n 1172, M_w 1371, M_w/M_n 1.17; elemental analysis (%) found (calcd.): C 41.1(41.3), H 2.4 (2.3), and N 8.3 (8.0).

Synthesis of OAPS

Five grams of ONPS (3.86 mmol), 50 mg $FeCl_3$, and 4 g active charcoal powder were charged into a three-necked 250 mL round-bottomed flask equipped with a mechanical stirrer and a condenser. THF (40 mL) was then added to the flask. The solution was stirred and heated to 60°C under N_2.

Hydrazine hydrate (16 mL) was added dropwise into the mixture. The reaction was continued for 4.5 h, and then the solution was cooled and filtered through Celite. The filtrate was combined with 25 mL of ethyl acetate and washed with H_2O thrice. The organic layer was dried over Na_2SO_4 and poured into 1 L petroleum ether. The white precipitate was collected by filtration. The product was redissolved in the mixture of 15 mL THF and 25 mL ethyl acetate, and reprecipitated into 500 mL petroleum ether. The obtained powder was dried in vacuum. The yield of the off-white OAPS was 86%.

FTIR (KBr): 3369, 3220 (w; N—H), 1119 cm^{-1} (s; Si—O—Si); GPC: M_n 1147, M_w 1330, and M_w/M_n 1.16; ^{29}Si solid NMR (δ, ppm): −70.0, −77.5; ^{1}H NMR (DMSO-d_6,) (δ, ppm): 7.8−6.0 (b, 2.0H), 5.3–3.7 (b, 1.0H). The product was soluble in THF, DMF, 1,4-dioxane, ethyl acetate, acetone, or DMSO and insoluble in benzene, ethanol, or water.

Preparation of BMI-DDE/OAPS nanocomposites

In formulating BMI-DDE/OAPS nanocomposites, the molar ratio of maleimide groups (in BMI) to amine groups (in DDE and OAPS) was kept at 1/1. The amino group molar ratio of OAPS/DDE was varied from 0/1 to 0.7/0.3. Table I shows the formulations used for the various nanocomposites studied. OAPS and DDE powders were added into a three-necked flask and weighed. Anhydrous acetone (30 mL) was added to dissolve the powders, with stirring. BMI (7.0 mmol) was then added to the solution. The mixture was refluxed with stirring under nitrogen for 6 h. After cooling, the acetone was removed by a rotary evaporator. The resulting brown product was further dried under reduced pressure and then grounded using an alumina mortar and pestle. The obtained

TABLE I
DSC and TGA Results of the BMI-DDE/OAPS Polyimides

OAPS/DDE[a]	OAPS content in polyimides (wt %)	T_g (°C)	T_{d1} (°C)	T_{d2} (°C)	Y_c (%)
0/1	0	195	317	364	35
0.3/0.7	15	231	329	381	42
0.5/0.5	24	224	357	388	45
0.7/0.3	33	201	376	399	53

[a] OAPS/DDE is defined as the amino group molar ratio of OAPS to DDE.

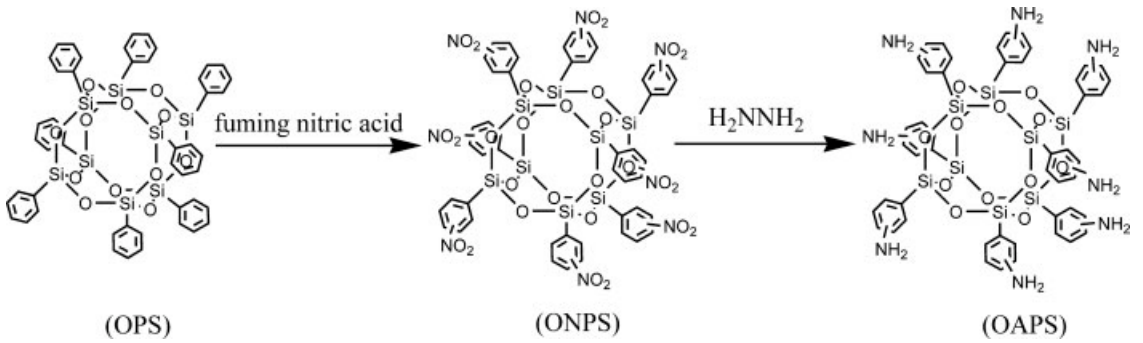

Scheme 1 Syntheses of ONPS and OAPS.

powder (2.5 g) was sealed in glass ampoule under nitrogen atmosphere. Polymerization of the sample was carried out by gradually increasing the temperature as follows: 150°C for 2 h, 200°C for 2 h, 250°C for 2 h, and 280°C for 30 min. The resulting clear and brown cured polymer was removed and grounded to a fine powder for characterization.

Measurement and characterization

FTIR spectra were obtained with Nexus 670 (FTIR) instrument. ^{1}H NMR and ^{29}Si solid state NMR spectra were recorded on a Bruker AV300 MHz spectrometer. Elemental analyses were performed on Flash EA 1112 automatic elemental analyzer. Molecular weight polydispersities were determined by a Waters515-2410 GPC, H3 + H5 + H6E μ-styragel columns and calibrated with standard polystyrene, using THF as the eluent. Glass transition temperature (T_g) was determined with a PerkinElmer Pyris-1 differential scanning calorimeter (DSC) with a heating rate of 20°C/min under N_2 atmosphere. Thermogravimetric analysis (TGA) was performed on a PerkinElmer TGS-2 with a heating rate of 20°C/min under N_2 atmosphere. Powder X-ray diffraction (XRD) was recorded with a D/Max 2500 VB2+/PC based analytical diffractometer using Ni-filtered Cu Kα radiation.

RESULTS AND DISCUSSION

Characterization of OAPS prepared by hydrazine hydrate reducing agent

The OAPS was prepared as depicted in Scheme 1, and its structure was characterized. In the FTIR spectrum of ONPS (Fig. 1), the two strong peaks at 1350 and 1529 cm^{-1} are assigned to sym. and asym. νN=O. But these two peaks disappeared after reduction as shown in the FTIR spectrum of OAPS, denoting the reduction reaction was complete. And new broad peaks appear at 3369 and 3220 cm^{-1}, which are assigned to νNH.[10,23]

In the ^{1}H NMR spectrum of OAPS (Fig. 2), no peak at 8–9 ppm corresponding to the protons in aromatic groups of ONPS was observed, while the aromatic hydrogens of OAPS were detected at higher magnetic field (7.8–6.0 ppm) due to the electron donor properties of amino groups on phenyl rings. This result indicated that the reduction reaction of nitro groups in

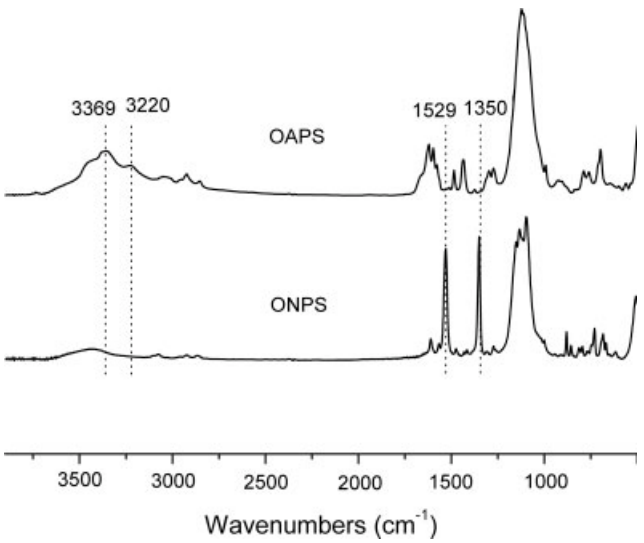

Figure 1 FTIR spectra of OAPS and ONPS.

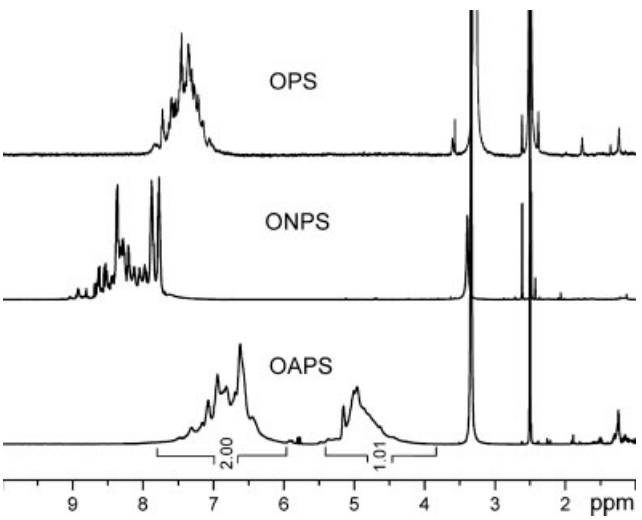

Figure 2 ^{1}H NMR spectra of OPS, ONPS, and OAPS.

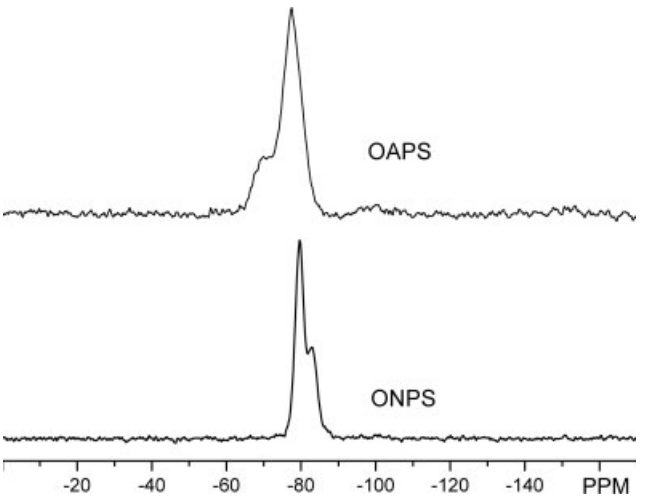

Figure 3 ^{29}Si NMR spectra of ONPS and OAPS.

ONPS by hydrazine hydrate was complete. The integration ratio of the peaks originating from protons in aromatic groups (7.8–6.0 ppm) and amino groups (5.3–3.7 ppm) of OAPS was equal to 2.00 : 1.01. This result indicated that one hydrogen atom per phenyl in OPS was substituted by nitro group forming ONPS, which was subsequently converted into amine group forming OAPS by reduction reaction.

The Si—O—Si bonds in silsesquioxane cages of OAPS could be characterized by the stretching bands at 1119 cm^{-1} in FTIR spectrum (Fig. 1).[18,23] The ^{29}Si solid NMR spectrum of ONPS shows two peaks at −79.5 and −82.8 ppm for the para and meta isomers, respectively (Fig. 3). Likewise, ^{29}Si solid NMR spectrum of OAPS also shows two respective peaks at −77.5 and −70.0 ppm, which are similar to those of OAPS prepared by the conventional method using Pd/C catalyst.[10,23] The cubic silsesquioxane structure was also confirmed by XRD study (Fig. 5, pattern a). A clear diffraction peak at $2\theta = 8^\circ$ ($d = 1.1$ nm, by Bragg's equation) corresponds roughly to the diameter of the OPS cage (1–1.1 nm), as pointed out by Choi et al.[14] The broad halo centered at $2\theta = 19^\circ$ is typical for an amorphous material, which arises because of the presence of amine substitutional isomers haphazarding the packing at molecular level. The narrow polydispersity of OAPS we prepared (Fig. 4, $M_w/M_n = 1.16$) also indicated the absence of oligomeric materials resulting from cage decomposition.[10,15] All the above-mentioned results indicate that OAPS prepared by hydrazine reducing agent retains the cage structure carrying eight amino-phenyl groups.

In addition, we also found that if the nitration time for preparing ONPS reached 10 and 20 h, the integration ratios of aromatic protons C—H to N—H protons in resulting OAPS products were 2.00 : 1.08 and 2.00 : 1.14, respectively, which were slightly lower than that of OAPS (2.00 : 1.01) we prepared. This result may suggest that some partial double nitration may have occurred during the long nitrifying period (20 h) for conventional ONPS preparation. The phenomenon of double nitration was also pointed out in literatures.[9] To confirm that the time for complete nitration could be shortened to 6 h, we characterized the ONPS product nitrified in 6 h by ^{1}H NMR, elemental analysis, and GPC. In ^{1}H NMR spectrum of OPS (Fig. 2), the aromatic hydrogen protons were detected at 7.0–7.8 ppm. However, in the spectrum of ONPS, the peaks corresponding to aromatic hydrogen protons were found only at the lower magnetic field (7.8–8.9 ppm), due to the electro-withdrawing effects of nitro groups on aromatic rings of ONPS. The elemental analysis data of ONPS agreed with the calculated values. All these results indicated the complete nitration for ONPS. The narrow polydispersity by GPC (Fig. 4, $M_w/M_n = 1.17$) confirmed the purity of ONPS.

Preparation and structural characterization of the BMI-DDE/OAPS nanocomposites

It was noted that OAPS possessing eight corner amino groups could behave as nanosized, rigid inorganic crosslinker in the bismaleimide-diamine polymerization system. Thus, introduction of OAPS into bismaleimide-dimaine resin may improve the thermomechanical stabilities of the resulting product. We prepared BMI-DDE/OAPS nanocoposites as depicted in Scheme 2. Mainly two reactions occured in BMI-diamine system at high temperature: BMI–BMI double-bond polymerization and BMI-diamine Michael

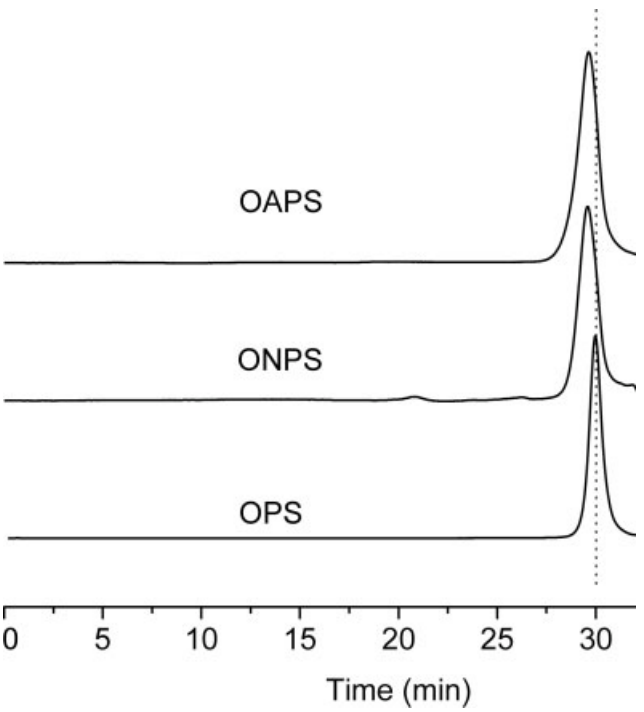

Figure 4 GPC traces of OAPS, ONPS, and OPS.

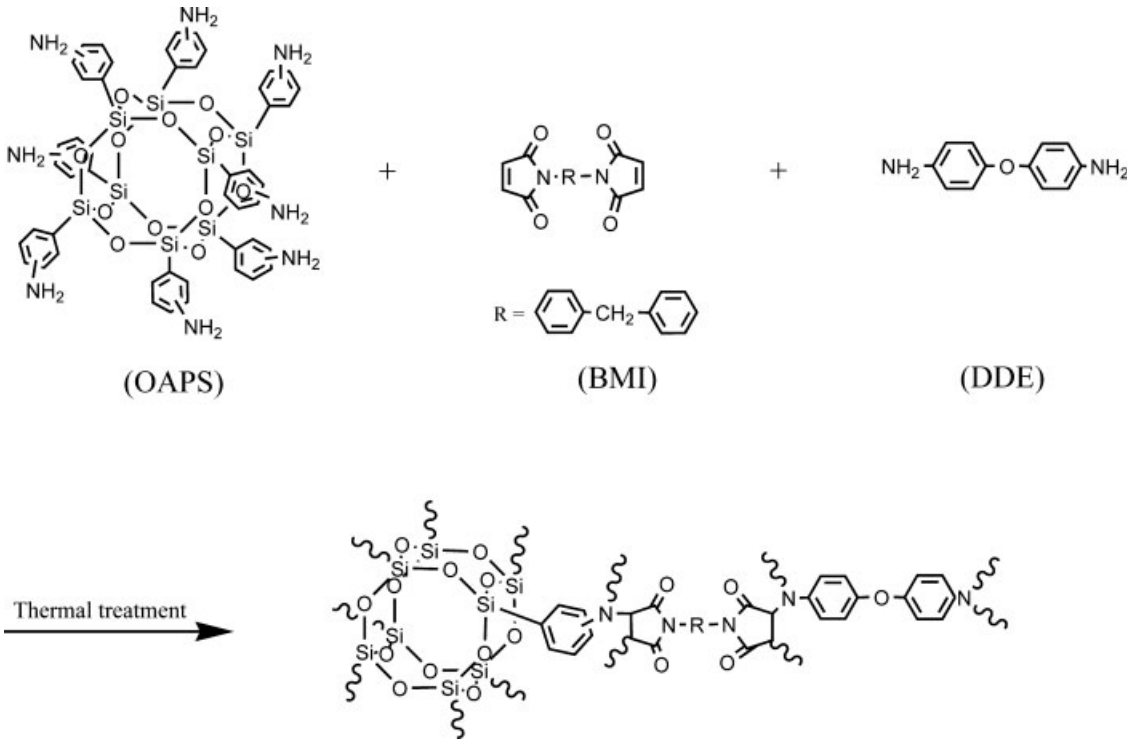

Scheme 2 Synthesis of BMI-DDE/OAPS nanocomposite.

addition reaction. The Michael addition of BMI and diamine leads to the formation of a secondary amine, which may react with another BMI molecule at higher temperature resulting in a crosslinked network.[24] The commonly held view is that the Michael addition reaction predominates at lower temperature (<180°C), and at higher temperature the homopolymerization reaction of BMI occurs at a comparable rate.[20,25,26] To get the well crosslinked polyimide, Wu et al.[21] preferred the curing temperature up to 280°C, which was followed in our study.

The BMI-DDE/OAPS nanocomposites were characterized by XRD and FTIR. Figure 5 displays XRD patterns for pure OAPS, BMI-DDE/OAPS nanocomposites with different OAPS content and control BMI-DDE polyimide. There is a clear peak at $2\theta = 8^\circ$ and an amorphous halo centered at $2\theta = 19^\circ$ in the diffraction pattern of OAPS. However, the clear peak, which is related to the long-range order in OAPS[18] disappeared from the patterns of cured polyimides, indicating the OAPS dispersion into polyimide. The XRD patterns of BMI-DDE/OAPS nanocomposites show

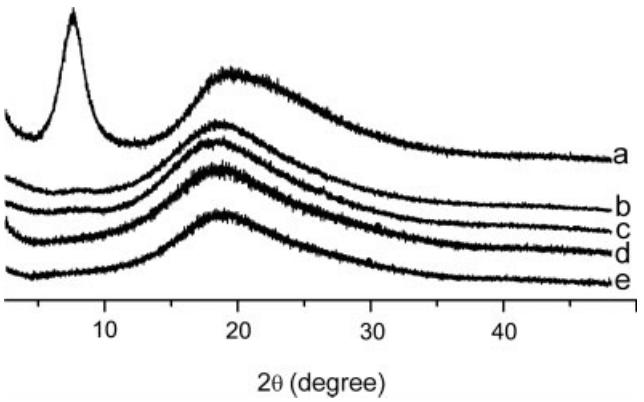

Figure 5 XRD patterns of BMI-DDE/OAPS polyimide. The different content of OAPS in polyimides (a), (b), (c), (d), and (e) are 100, 33, 24, 15, and 0 wt %, respectively.

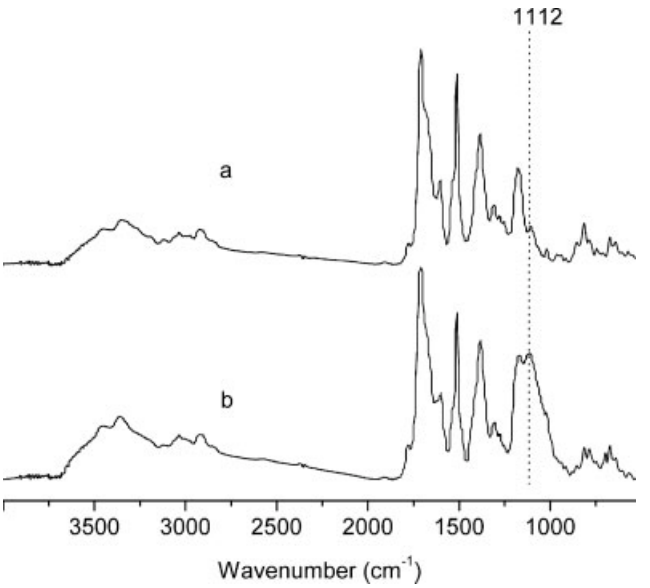

Figure 6 FTIR spectra of BMI-DDE/OAPS polyimides. The OAPS content in polyimides (a) and (b) are 0 and 24 wt %, respectively.

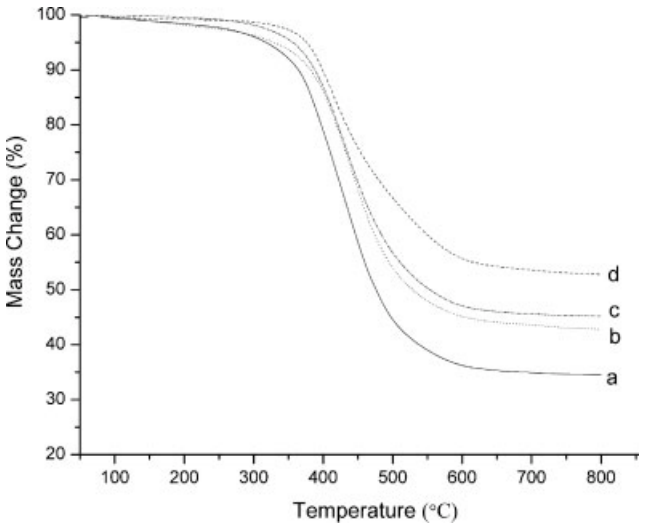

Figure 7 TGA curves of the BMI-DDE/OAPS nanocomposites. The different content of OAPS in polyimides (a), (b), (c), and (d) are 0, 15, 24, and 33 wt %, respectively.

only the weak amorphous peaks centered at $2\theta = 19^\circ$, the intensities of which are quite similar to that of control BMI-DDE polyimide prepared without OAPS loading and do not change as the OAPS content increased. This finding indicates that the amorphous peaks in composites are mainly due to the control polyimide, implying that OAPS is dispersed into the polyimide network as compatible and unassociated POSS units, as suggested by Liang et al.[27] in the study on cyanate ester/POSS nanocomposite.

The preservation of inorganic cube structure in the nanocomposites after curing at high temperature could be verified by the strong νSi—O (cube) peak in FTIR spectra at 1112 cm^{-1}, which is used as an internal reference for the composites.[14,18] This peak was absent for the polyimide without OAPS loading (Fig. 6).

The thermal analysis of BMI-DDE/OAPS nanocomposites

The effect of OAPS on the T_g values of the BMI-DDE systems was examined by DSC. In our results (Table I), the T_g of BMI-DDE/OAPS nanocomposite was enhanced by 36°C with OAPS content around 15 wt %. However, as the feed amount of OAPS increased further, the decrease in T_g's could be observed. This phenomenon can be explained by the fact that there are two competitive factors determining the T_g's of resulting materials. On one hand, the hindering effect of POSS cubes on polymer chain motions enhances the T_g. On the other hand, the increase in free volume of the system due to the inclusion of the bulky POSS cubes decreases the T_g.[23] All the T_g values with incorporating the OAPS into the system were higher than that of control sample without OAPS loading.

The TGA data of BMI-DDE/OAPS nanocomposites are shown in Table I and Figure 7. As the OAPS loading increased from 0 to 34 wt %, the values of 5 and 10% mass loss temperature (T_{d1} and T_{d2}) increased by 59 and 35°C, respectively, indicating that the cured nanocomposites have excellent thermal stability. The char yields (Y_c, 800°C) evaluated by TGA also increased with increasing OAPS loading. High char yields are a direct indication of resistance to combustion. The improved thermal stabilities and flame retardence of BMI-DDE/OAPS nanocomposites are likely due to the combined effects of the cubic silica cores, the stable imide tethers and higher crosslinking densities, which retarded diffusion of gaseous fragment products during decomposition.[19]

CONCLUSIONS

This article describes a novel and facile way for preparation of OAPS by using stable, inexpensive, and readily available hydrazine hydrate as reducing agent with a yield of 86%. The OAPS containing the inorganic cube cage and one amino group on each aromatic ring was characterized by FTIR, NMR, XRD, GPC, and TGA. To avoid the double nitration of ONPS prepared by the conventional way, we shortened the nitrifying time from 20 to 6 h and examined the structure of the product by ^{1}H NMR and elemental analysis. Novel BMI-DDE/OAPS nanocomposites were prepared through Michael addition reaction. The preservation of inorganic cubes and their dispersion in the cured nanocomposites were characterized by XRD and FTIR. The resulting nanocomposites exhibited improved thermal properties and flame retardence. The T_g value of nanocomposite was enhanced by 36°C with the OAPS loading around 15 wt %, but as the feed amount of the OAPS increased further, the decrease in T_g's could be observed. All the T_g values of nanocomposites were higher than that of the control sample without the OAPS loading.

References

1. Baney, R. H.; Itoh, M.; Sakakibara, A.; Suzuki, T. Chem Rev 1995, 95, 1409.
2. Mi, Y.; Stern, S. A. J Polym Sci Part B: Polym Phys 1991, 29, 389.
3. Lee, Y. J.; Huang, J. M.; Kuo, S. W.; Lu, J. S.; Chang, F. C. Polymer 2005, 46, 173.
4. Gilman, J. W.; Schlitzer, D. S.; Lichtenhan, J. D. J Appl Polym Sci 1996, 60, 591.
5. Choi, J.; Yee, A. F.; Laine, R. M. Macromolecules 2003, 36, 5666.
6. Kim, G. M.; Qin, H.; Fang, X.; Sun, F. C.; Mather, P. T. J Polym Sci Part B: Polym Phys 2003, 41, 3299.
7. Pellice, S. A.; Fasce, D. P.; Williams, R. J. J. J Polym Sci Part B: Polym Phys 2003, 41, 1451.
8. Mya, K. Y.; He, C.; Huang, J.; Xiao, Y.; Dai, J.; Siow, Y. P. J Polym Sci Part A: Polym Chem 2004, 42, 3490.

9. Kim, S. G.; Choi, J.; Tamaki, R.; Laine, R. M. Polymer 2005, 46, 4514.
10. Tamaki, R.; Tanaka, Y.; Asuncion, M. Z.; Choi, J.; Laine, R. M. J Am Chem Soc 2001, 123, 12416.
11. Jeon, H. G.; Mather, P. T.; Haddad, T. S. Polym Int 2000, 49, 453.
12. Lee, A.; Lichtenhan, J. D. J Appl Polym Sci 1993 1999, 73.
13. Li, G.; Wang, L.; Ni, H.; Pittman, C. U., Jr. J Inorg Organomet Polym 2001, 11, 123.
14. Choi, J.; Tamaki, R.; Kim, S. G.; Laine, R. M. Chem Mater 2003, 15, 3365.
15. Huang, J. C.; He, C. B.; Xiao, Y.; Mya, K. Y.; Dai, J.; Siow, Y. P. Polymer 2003, 44, 4491.
16. Liu, H.; Zhang, W.; Zheng, S. Polymer 2005, 46, 157.
17. Ni, Y.; Zheng, S.; Nie, K. Polymer 2004, 45, 5557.
18. Tamaki, R.; Choi, J.; Laine, R. M. Chem Mater 2003, 15, 793.
19. Choi, J.; Kim, S. G.; Laine, R. M. Macromolecules 2004, 37, 99.
20. Curliss, D. B.; Cowans, B. A.; Caruthers, J. M. Macromolecules 1998, 31, 6776.
21. Wu, W.; Wang, D.; Ye, C. J Appl Polym Sci 1998, 70, 2471.
22. Lin, K. F.; Lin, J. S.; Cheng, C. H. Polymer 1996, 37, 4729.
23. Ni, Y.; Zheng, S. Chem Mater 2004, 16, 5141.
24. Okumoto, S.; Yamabe, S. J Org Chem 2000, 65, 1544.
25. Tung, C. M. Polym Prepr 1987, 28, 7.
26. Tungare, A. V.; Martin, G. C. J Appl Polym Sci 1992, 46, 1125.
27. Liang, K.; Toghiani, H.; Li, G.; Pitterman, C. U., Jr. J Polym Sci PartA: Polym Chem 2005, 43, 3887.